Numerical Analysis on Turbulence and Air-Water Scalar Transport in Open-Channel Flow Influenced by Thermal Stratification and Surface Shear Stress

Kim, SungJin
Interdisciplinary Graduate School of Engineering Sciences, Kyushu University

Sugihara, Yuji
Interdisciplinary Graduate School of Engineering Sciences, Kyushu University

Eljamal, Osama
Interdisciplinary Graduate School of Engineering Sciences, Kyushu University

https://doi.org/10.5109/4102490

出版情報：Proceedings of International Exchange and Innovation Conference on Engineering & Sciences (IEICES). 6, pp.212-218, 2020-10-22. Interdisciplinary Graduate School of Engineering Sciences, Kyushu University

Numerical Analysis on Turbulence and Air-Water Scalar Transport in Open-Channel Flow Influenced by Thermal Stratification and Surface Shear Stress

SungJin Kim[1], Yuji Sugihara[1] and Osama Eljamal[1]
[1]Interdisciplinary Graduate School of Engineering Sciences, Kyushu University
Corresponding author email: user0galaxy@gmail.com

ABSTRACT: *It is important for estimating accurately the air-water transport of scalar such as heat and gas to understand turbulent characteristics close to the water surface. Near-surface turbulence in natural hydro-environments is influenced by the thermal stratification and the wind shear stress acting on the water surface. The purpose of this study is to numerically investigate how their factors influence the turbulent structure and the air-water scalar transport in an open channel flow by means of the direct numerical simulation, i.e., DNS. We reproduce the combined effects of the thermal stratification and the surface shear stress on the structure of the turbulent flow and the scalar transport on the water surface. The numerical results suggest that the scalar transport velocity is obviously changed by the combined effects of the thermal stratification and the surface shear stress.*

Keywords: Thermal stratification; surface shear stress; open-channel flow; surface divergence; DNS

1. INTRODUCTION

1.1 Background

Turbulent conditions at the water surface have a great influence on the transport of scalar such as heat and gas. In natural hydro-environments, there are some factors that change the near-surface turbulence, e.g., the wind stress acting on the water surface, the solar radiation and the radiative cooling and so on. The wind stress on the water surface affects effectively the near-surface structure of turbulence because it generates the strong vertical velocity shear near the water surface. In addition, the solar radiation and the radiative cooling can change the thermal vertical stratification, for which there exist two types, i.e., stable stratification caused by the solar radiation and unstable stratification caused by the radiative cooling. In order to evaluate accurately the scalar transport velocities in flow fields with the somewhat strong temperature variation of fluid, it is necessary to consider the effect of the thermal stratification on a turbulent flow field. Scalar transports across the water surface can be recognized as turbulent phenomena at spatially and temporally micro scales. We may expect a universal mechanism for the air-water scalar transport controlled by micro-scale turbulent motions, independent of types of flow fields. Turbulence characteristics connected with the thermal stratification or the surface shear stress have been investigated individually in previous research works.

Several theoretical and experimental models have been proposed to define the scalar transport velocity such as the gas transfer velocity at the water surface. Their models have been roughly classified into the surface divergence model, small eddy model (SEM) and large eddy model (LEM). Sanjou and Nezu [1] measured the surface divergence under hydraulic conditions changing the depth in open-channel flows. They described that the gas transfer velocity for open-channel flows of comparatively shallow depth does not agree with the surface divergence model from existing studies. Hasegawa and Kasagi [2] proposed a hybrid numerical model combining DNS and large eddy simulation (LES), and compared the scalar transport velocity at low and high Schmidt numbers. Herlina and Jirka [3] carried out laboratory experiments on the gas transfer at the air-water interface induced by oscillating-grid turbulence by means of a particle image velocimetry, i.e., PIV. Their results suggested that small eddies and large eddies play important roles to determine the gas transfer velocity. Also, Herlina and Wissink [4] executed the direct numerical simulation, i.e., DNS, under numerical conditions ranging from low Reynolds number to high Reynolds number. From this research, it was suggested that though the gas transfer velocity obeys LEM at low value of Reynolds number, whereas in the case of high value the transfer velocity follows SEM.

Komori et al. [5] conducted a laboratory experiment for turbulent open-channel flows under stable stratification, and they revealed that turbulence statistics in such flows depends on a local Richardson number defined by the local flow velocity and temperature gradient. In addition, Komori et al. [6] also carried out DNS for open-channel turbulence and passive scalar transport. The numerical results demonstrated that the surface-renewal eddies are due to that the bursting phenomenon close to the bottom reach the water surface, and the scalar transport at the water surface is promoted by such renewal eddies. Nagaosa et al.[7] examined the time scale of turbulent vortices controlling the scalar transfer, and compared it with the fluctuation cycle of the dissolved gas concentration measured by Komori et al.[8]. Dong and Lu[9] attempted to make DNS for open channel turbulence at a wide range of Richardson number including unstable stratification conditions, and investigated numerically the turbulence characteristics and the dependence of Nusselt number on Richardson number. Teraoka et al.[10] carried out the direct numerical simulation of open-channel turbulence incorporating the thermal stratification, and analyzed how the thermal stratification influences turbulence characteristics on the water surface. They also confirmed that the surface divergence of the horizontal velocities and the heat flux on the water surface vary depending on stable and unstable stratifications.

We should consider how the combination of the thermal stratification and the surface shear stress influences turbulent characteristics close to the water surface. However, attempts for examining the combination effects are quite unique and complex, and thus we have no enough knowledge about the interaction between both effects.

The scalar flux on the water surface F can be expressed by the product of the scalar transport velocity k_L and the concentration difference ΔC between the water surface C_s and that the bulk water C_b as follows:

$$F = k_L (C_S - C_b) = -D \left. \frac{\partial C}{\partial y} \right|_{surface} \quad (1)$$

where y denotes the vertical coordinate and D the molecular diffusivity of scalar. In order to calculate the air-water scalar flux, the transport velocity must be quantitatively evaluated though it should depend on the thermal stratification and the surface shear stress. It is an interesting research in fluid dynamics to investigate how turbulent properties and the air-water scalar transport vary with both effects of the thermal stratification and the surface shear stress.

1.2 Purpose of this study

The purpose of this study is to investigate the effects of the thermal stratification and the surface shear stress on the scalar transport in an open-channel flow by means of the direct numerical simulation, so-called DNS, which is a numerical method to solve directly all turbulent eddies existing in a flow field without including any turbulence closure models. The effect of the thermal stratification seems to induce convective flows and the suppression of vertical mixing, so that turbulence characteristics should be greatly changed. Our analytical target is an open-channel flow including the effects of the thermal stratification and the surface shear stress. The open-channel flow is well known as one of the simplest flow fields, including the essential properties of turbulence, and thus it is possible to understand simply the physical mechanism of the air-water scalar transport. Their effects on the turbulent properties and the scalar transport are examined through the numerical analysis.

2. OUTLINE OF NUMERICAL SIMULATION

2.1 Basic equations

The basic equations in the numerical simulation are the continuity equation of incompressible fluid, the heat transport equation, and the Navier-Stokes equation under Boussinesq approximation, which is possible to neglect the density change exception in the gravitational term in the Navier-Stokes equation. Under this approximation, the change in density only affects the motion of fluid through the buoyancy force in proportion to gravity. The basic equations are expressed as follows:

・Continuity equation

$$\frac{\partial u_i^*}{\partial x_i^*} = 0 \quad (2)$$

・Heat transport equation

$$\frac{\partial T^*}{\partial t^*} + u_j^* \frac{\partial T^*}{\partial x_j^*} = \frac{1}{PrRe_\tau} \left(\frac{\partial^2 T^*}{\partial x_j^* \partial x_j^*} \right) \quad (3)$$

・Navier-Stokes equation under Boussinesq approximation

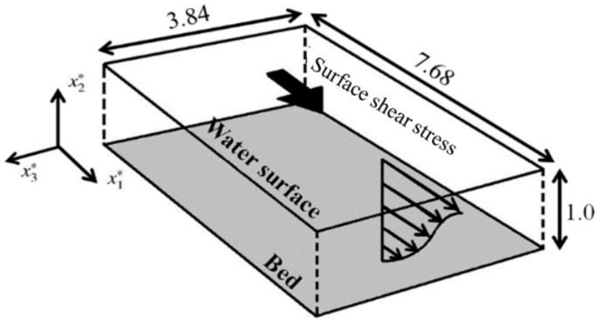

Fig. 1. Schematic diagram of computational domain.

Table 1. Computational conditions

Calculation area		Main direction x_1^* : 7.68	
		Vertical direction x_2^* : 1.0	
		Span direction x_3^* : 3.84	
Grid points		$(N_{x1}, N_{x2}, N_{x3}) = (128, 129, 128)$	
Grid space		Δx_1^* : 0.06	
		Δx_2^* : $7.4\text{x}10^{-4} \sim 1.5\text{x}10^{-2}$	
		Δx_3^* : 0.03	
Time interval		$\Delta t^* = 5.0\text{x}10^{-5}$	
Parameters		$Re_\tau = 150$, $Fr_\tau = 1 - \tau_s^*$, $Pr = 1$	
		$Ri_\tau = -5, 0, 5$	
		$\tau_s^* (\equiv \tau_s / \tau_b) = -0.3, 0, 0.3$	
Boundary conditions		x_1^*, x_3^*	x_2^*
Flow velocity	u_1^*, u_3^*	Periodic boundary conditions	$x_2^* = 1$: Neumann
			$x_2^* = 0$: Dirichlet
	u_2^*		Dirichlet
Pressure			Neumann
Temperature			Dirichlet

$$\frac{\partial u_i^*}{\partial t^*} + u_j^* \frac{\partial u_i^*}{\partial x_j^*} = -\frac{\partial p^*}{\partial x_i^*} + \frac{1}{Re_\tau} \left(\frac{\partial^2 u_i^*}{\partial x_j^* \partial x_j^*} \right) + \frac{\delta_{1i}}{Fr_\tau^2} + |Ri_\tau| T^* \delta_{2i} \quad (4)$$

The above equations have been non-dimensionalized with the depth H, the bottom friction velocity u_τ, and the temperature difference between the water surface and the bottom, i.e., $\Delta T(=T_s-T_0)$. The indication of * denotes the non-dimensional quantity. Dimensionless parameters controlling the state of flow are Reynolds number $Re_\tau (\equiv u_\tau H/\nu)$, Froude number Fr_τ $(\equiv u_\tau/\sqrt{gHsin\theta})$, Richardson number Ri_τ $(\equiv \alpha \Delta T g \cos\theta H/u_\tau^2)$, the non-dimensional surface shear stress $\tau_s^* (\equiv \tau_s / \tau_b)$ and Prandtl number $Pr(\equiv \nu/\kappa)$, with ν, $\sin\theta$, κ, α, g, τ_s and τ_b being the kinematic viscosity, the bottom slope of the channel, the temperature diffusion coefficient, the coefficient of thermal expansion, the gravitational acceleration, the shear stress on the water surface, i.e., the surface shear stress, and the shear stress on the bottom, respectively.

2.2 Computational conditions

Figure 1 shows a schematic diagram of the computational domain in the present numerical simulation. The target

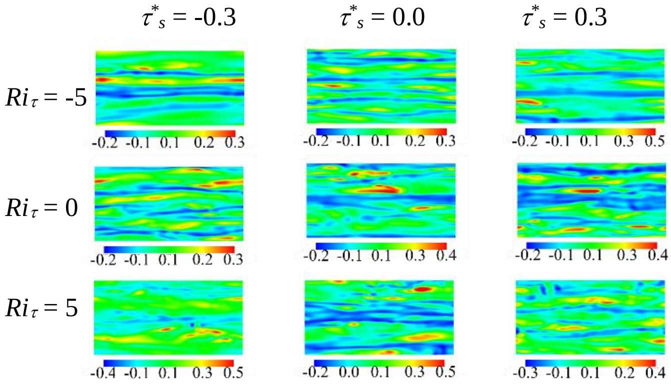

Fig. 2. Turbulence structures near the bottom.

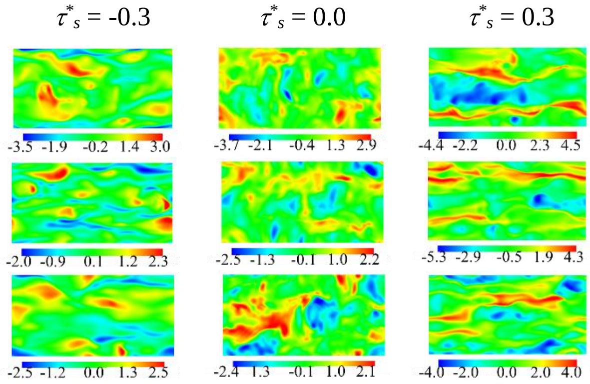

Fig. 3. Turbulence structures near the water surface.

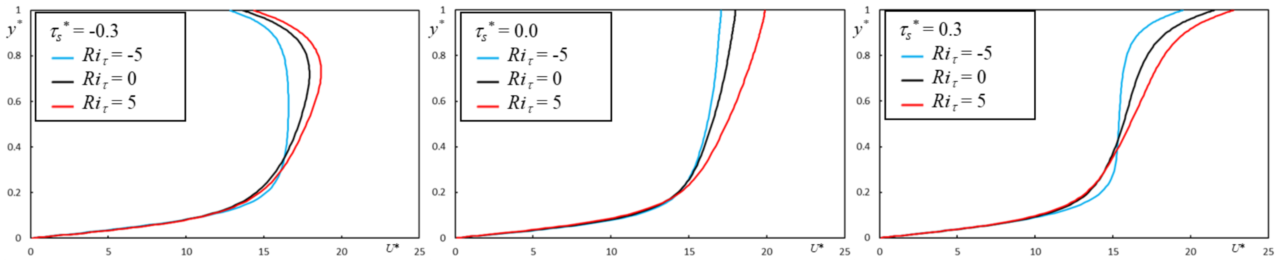

Fig. 4. Vertical profiles of the mean longitudinal velocity.

of the simulation is an open-channel flow. The non-slip condition is imposed on the bottom surface, and the water surface is the flat surface with no deformation. For the coordinate axes in each direction, the longitudinal axis is defined to be x_1^*, the vertical direction x_2^* is taken upward from the bottom, and the spanwise direction becomes x_3^*. It should be noted that in the later figures, x_2^* is indicated by y^* because of simplification.

Table 1 gives the computational conditions in this simulation, where the value of Reynolds number defined on the basis of the bottom friction velocity is fixed at 150. The relation of Froude number with Reynolds number in the table is because the statistical steady flow forms in the equilibrium state between the bottom friction, the gravitational force and the surface shear stress. The values of Richardson number of -5, 0 and 5 mean unstable, neutral, and stable stratifications, respectively. Also, Prandtl number is fixed to be unity from viewpoint of calculation's simplicity. The dimensionless surface shear stress is changed to -0.3, 0 and 0.3 in this simulation. The vertical boundary conditions for the velocities are as follows:

$$u_1^* = u_2^* = u_3^* = 0 \quad \text{at bottom} \tag{5}$$

$$\frac{1}{Re_\tau}\frac{\partial u_1^*}{\partial x_2^*} = \tau_s^*, \quad u_2^* = 0, \quad \frac{\partial u_3^*}{\partial x_2^*} = 0 \quad \text{at water surface} \tag{6}$$

Also, the periodic boundary conditions are imposed in longitudinal and spanwise directions. In the case of the neutral condition, the passive heat transport is analyzed under no buoyancy term in the equation of motion.

3. RESULTS AND DISCUSSION

3.1 Turbulence structures influenced by thermal stratification and surface shear stress

Figure 2 shows examples of streaky turbulence structures near the bottom under the respective conditions, which are visualized by the spatial fluctuation of the longitudinal velocity. In the vicinity of the bottom turbulent boundary layer, there exists a streaky coherent structure, so-called the low speed streak for which low speed regions are arranged like lines in the longitudinal direction. They are one of typical coherent structures in the wall boundary layer turbulence, and play an important role in the regeneration process of vortices near the bottom[11]. It is natural to consider that similar streaky structures appear near the sheared water surface, though the streaky structures near the bottom and the water surfaces may have different properties. In addition, the effects of the thermal stratification on the streaky structures are notable from viewpoint of fluid dynamics.

Figure 3 shows the structures of the near-surface turbulence visualized by the spatial fluctuation of the longitudinal velocity in the vicinity of the water surface. When the surface shear stress is positive with respect to the flow direction, high speed streaks can be observed near the water surface. The spatial scale of such high-speed streaks increases with the decrease of Richardson number, and this is caused by the convective motion induced by the unstable stratification. On the other hand, in the case of the negative surface shear stress, the low speed streaks appear near the water surface. However, the spatial pattern seems to be somewhat indistinct in comparison with the low speed streaks observed near the bottom. The difference between both is caused by the mechanism of the stretching of the longitudinal vortices.

Figure 4 shows the vertical profiles of the mean longitudinal velocity simulated in this study. It can be seen from the figure that the mean surface flow velocity varies obviously depending on the values of τ^*_s and Ri_τ.

When the negative stress acts on the water surface, the mean surface velocity decreases, whereas it increases in

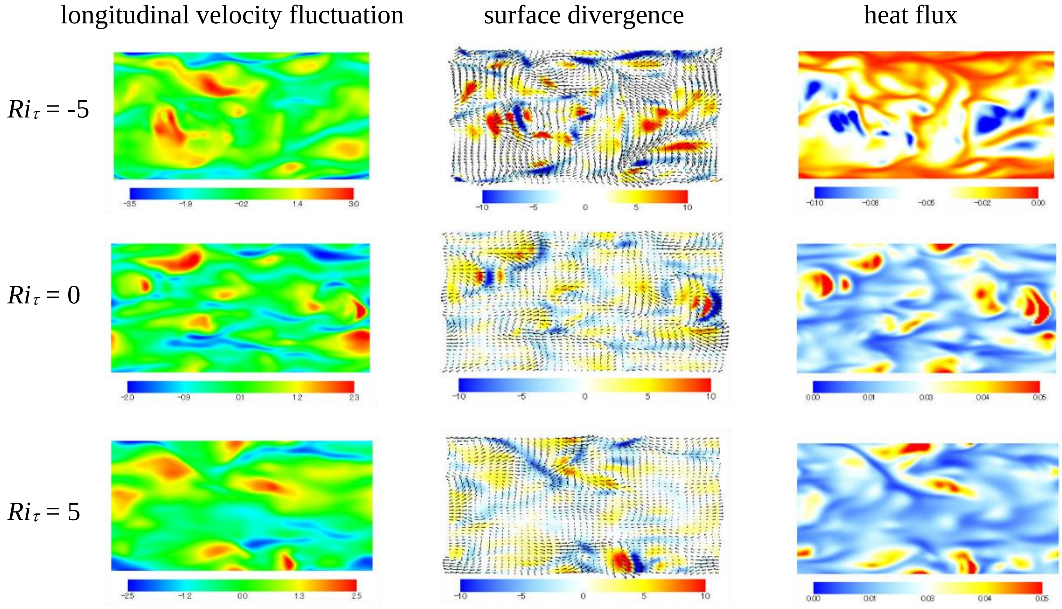

(a) τ^*_s = -0.3

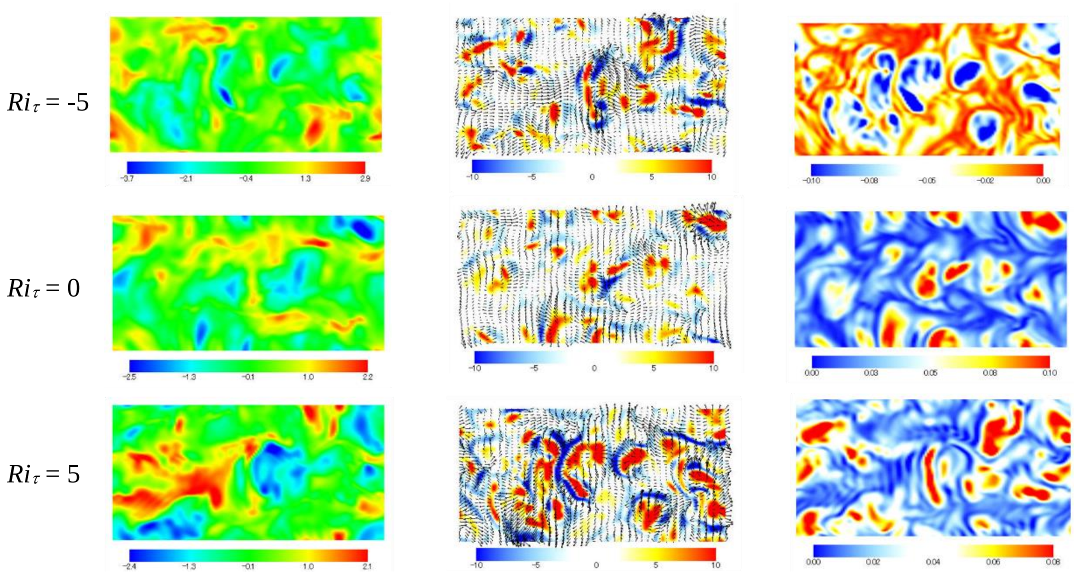

(b) τ^*_s = 0

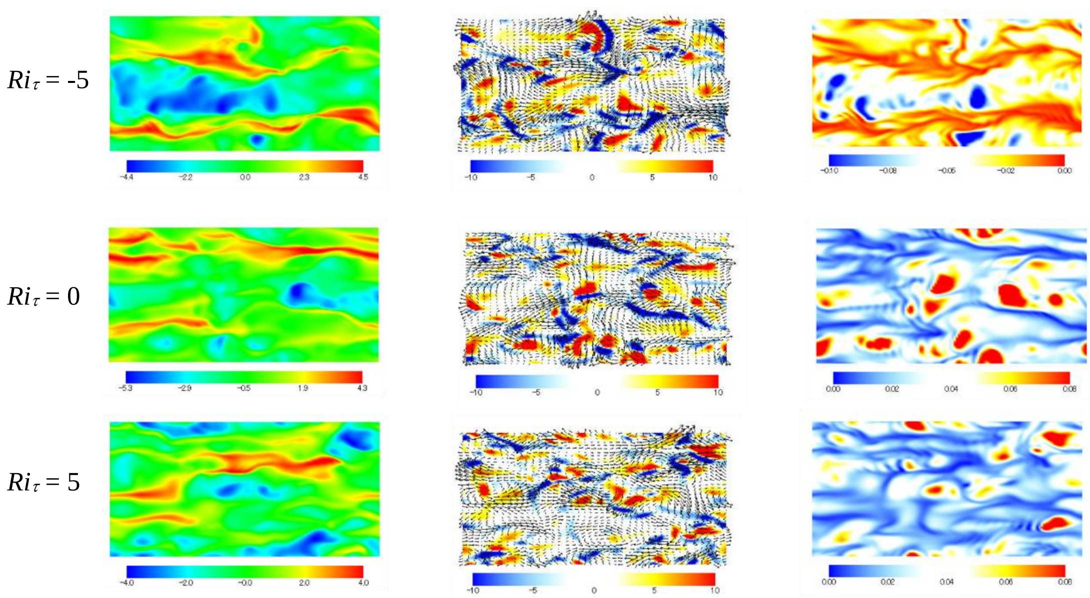

(c) τ^*_s = 0.3

Fig. 5 Spatial distributions of longitudinal velocity fluctuation, surface divergence and heat flux on the water surface

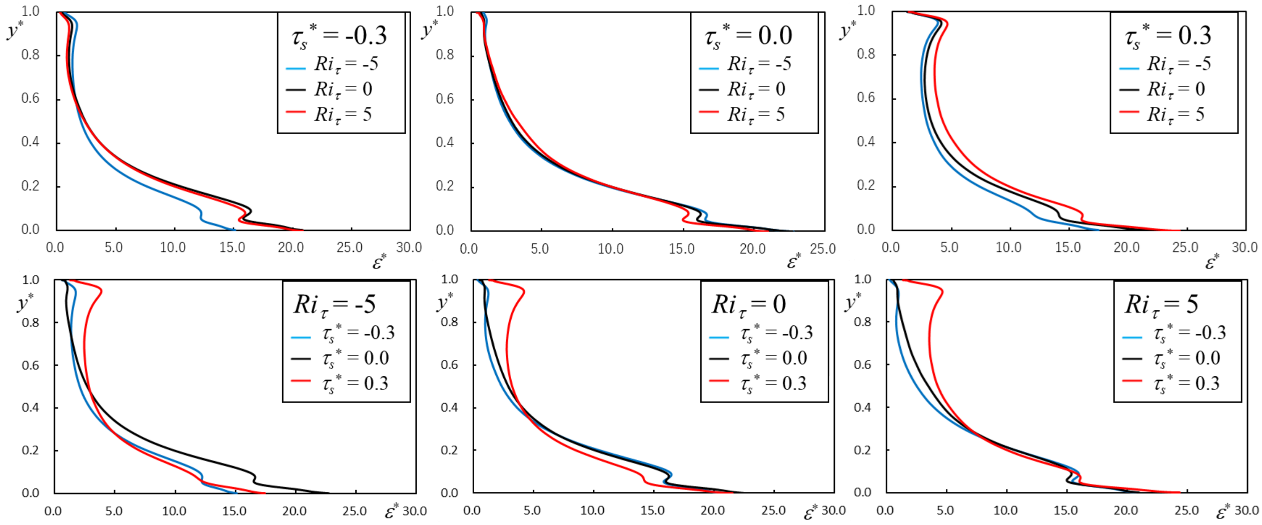

Fig. 6. Vertical profiles of dissipation rate of turbulent energy.

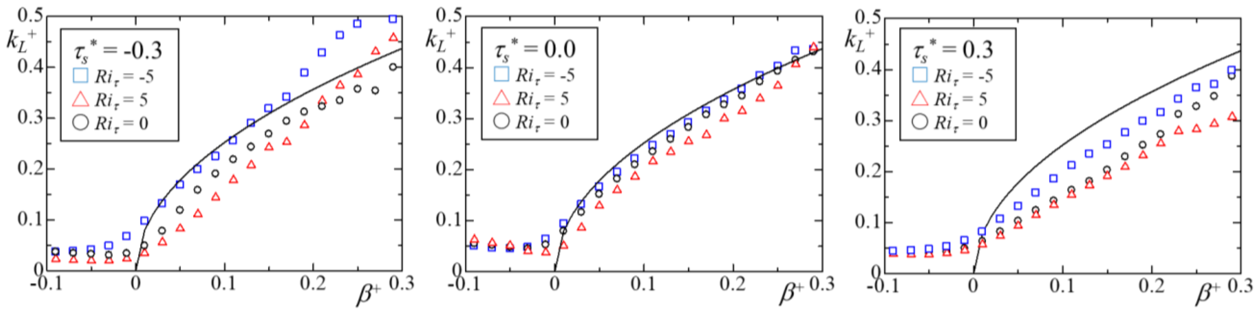

Fig. 7. Comparisons of analytical solution of local scalar transfer velocity with numerical results.

the case of the positive stress. In the case where the value of Ri_τ is negative, the velocity profile becomes homogeneous in the vertical direction by the convection due to the unstable stratification. On the other hand, when the value is positive, the vertical mixing of the momentum is found to be suppressed. For the positive and zero shear conditions, the longitudinal vortices generated close to the bottom can be stretched as they rise to the upper layer because its stretching direction is consistent with the surface velocity shear, whereas when the shear stress is negative, the vortex stretching from the bottom becomes opposite to the stretching near the water surface.

Turbulent motions close to the water surface may be directly related to the divergence of the horizontal velocities, hereafter we will call it the surface divergence. The surface divergence can be measured directly by a particle image velocimetry, so that it is recognized as an important dynamical quantity for describing the scalar transport on the water surface. The surface divergence is defined by

$$\beta^* = \left.\frac{\partial u_1^*}{\partial x_1^*} + \frac{\partial u_3^*}{\partial x_3^*}\right|_{surface} \tag{7}$$

In addition, the heat flux on the water surface is defined as follows:

$$F^* = \left.\frac{1}{PrRe_\tau}\frac{\partial T^*}{\partial x_2^*}\right|_{surface} \tag{8}$$

where the flux is defined to be positive in the downward direction.

Figures 5 (a) to (c) show the spatial distributions of the surface divergence and the heat flux on the water surface, comparing with the longitudinal velocity fluctuation, where the flux becomes negative in the case of unstable stratification, and the ranges of the scale bar are different between the respective figures. The region where the surface divergence is positive corresponds to the upward flow region, whereas the negative divergence corresponds to the downward flow one. In the neutral and stable stratification, the low scalar fluids rising from the lower layer reach the water surface and the interfacial scalar transport is driven by the surface renewal eddies. On the other hand, in the case of unstable stratification, the positive divergence drives the negative flux.

For the negative surface shear stress, the value of divergence becomes lower than that in the other cases of the shear stress. Also, the high speed regions on the water surface are found to be patch-shaped pattern, and the low speed ones become streaky. In the case of stable stratification, the spatial scale of the high flux region becomes relatively small because of the suppression of the vertical motion. For unstable stratification, the scale of the flow is increased by large-scale convective motions. For neutral condition, the obvious patch-shaped pattern is dominated on the water surface, whereas for stable stratification, the patch pattern becomes relatively unclear by the stabilization of momentum transfer in the vertical direction. It seems that the thermal stratification affects significantly the heat flux on the water surface. The divergent motion on the water surface makes the scalar boundary layer thin, so it is considered the heat transport increases accordingly. Comparing the surface divergence with the heat flux, we can see that in the cases of neutral and stable stratification, large areas of positive surface divergence corresponds to large areas of heat flux. Conversely, in the case of unstable stratification, the positive divergence region corresponds to the negative heat flux one. Thus, even when the turbulent structures are influenced by the thermal stratification and the surface shear stress, the surface divergence seems to be related to the scalar transport at the water surface.

The dissipation rate of the turbulent kinetic energy is an important parameter for understanding turbulence characteristics because the energy of turbulence is transferred from a large scale to a small scale eddies. The energy dissipation rate connects with the surface divergence, which is scaled by using the turbulent velocity and Taylor micro scale (see Tsumori and Sugihara[12]). Figure 6 shows the vertical profiles of the dissipation rate of the turbulent kinetic energy. The vertical profile under the conditions of τ^*_s=0 and Ri_τ=0 agrees with that provided from the previous numerical results. The energy dissipation rate in the case of the positive surface shear stress becomes larger than those in the other cases. This may be due to that the strong velocity shear is generated near the water surface. The profile takes a local maximum value in the surface layer. The behavior is observed in the case of the negative surface shear stress, but the local maximum value is relatively small. Based on the numerical results, varying with the value of Ri_τ under the condition of τ^*_s=0, the pure effect of the thermal stratification may be small compared to the surface shear stress though the combined effects of the stratification and the shear stress should be examined.

An analytical solution of the advection-diffusion equation for scalar under the stagnation-flow approximation has been frequently applied in comparison with the numerical results. The analytical solution of the scalar transport velocity is expressed by

$$k_L^+ = \sqrt{\frac{2}{\pi}} Sc^{-\frac{1}{2}} \sqrt{\beta^+} \qquad (9)$$

where + denotes the dimensionless quantity in the form of the wall unit. Figure 7 shows the relationships between the local scalar transport velocity and the local surface divergence, where the solid line obtained from Eq. (9) is also drawn in the figure for comparison of the numerical results with the analytical solution. It is seen from the figure that under the conditions of τ^*_s=0 and Ri_τ=0, the numerical results agree approximately with the analytical solution. In overall, the numerical results influenced by the surface shear stress become smaller than the line of the analytical solution. Also, the effect of the stratification on the scalar transport velocity may be changed in the order of Ri_τ=-5, 0, 5, which is due to that the thermal stratification influences a mechanism that the turbulence occurred near the bottom reach the water surface. From these figures, the scalar transport velocity should be modified on the basis of the combined effects of the thermal stratification and the surface shear stress.

4. CONCLUSIONS

In this study, we focused on the scalar transport at the water surface and analyzed the open-channel flow, including the effects of the thermal stratification and the surface shear stress by means of DNS. The numerical results showed that high speed streaky structures near the water surface appear under the conditions of the positive shear stress, and the spatial scale of the streaky structures depend on the thermal stratification. The positive surface divergence regions, showing the patch patterns were found to be closely connected with the surface heat flux on the water surface, but for stable stratification, the patch pattern becomes relatively unclear because the turbulence from the bottom is suppressed by the stabilization in the vertical direction. In addition, the effects of the thermal stratification and the surface shear stress on the dissipation rate of the turbulent kinetic energy were investigated, and the surface shear stress has a great impact on the vertical profile of the energy dissipation rate of the turbulent energy. It has been concluded from the present results that the scalar transport velocity should be modified by considering the combined effects of the thermal stratification and the surface shear stress.

ACKNOWLEDGMENTS

This work was partially supported by a Grant-in-Aid for Scientific Research (B) (Coordinator: Y. Sugihara, JSPS KAKENHI Grant Number JP19H02249).

3. REFERENCES

[1] Sanjou, M. and Nezu., Experimental study on surface velocity divergence and interfacial gas transfer in open-channel flows, Journal of JSCE, 1(2013), 82-89.
[2] Hasegawa, Y. and Kasagi, N., Hybrid DNS/LES of high Schmidt number mass transfer across turbulent air-water interface, J. Heat Mass transfer, 52(2009), 854-874.
[3] Herlina and Jirka, G. H., Experiments on the gas transfer at the air-water interface induced by oscillating grid turbulence, J. Fluid Mech., 594(2008), 183-208.
[4] Herlina H. and Wissink J.G., Direct numerical simulation of turbulent scalar transport across a flat surface, J Fluid Mech, 744(2014), 217-249.
[5] Komori, S., H. Ueda, F. Ogino and T. Mizushina, Turbulence structure in stably stratified open-channel flow, J. Fluid Mech., 130(1983) 13-26.
[6] Komori, S., Nagaosa, R. and Murakami, Y., Turbulence structure and mass transfer across a sheared air-water interface in wind-driven turbulence, J. Fluid Mech, 249(1993), 161-183.
[7] Nagaosa R., and R. A. Handler, Characteristic time scales for predicting the scalar flux at a free surface in turbulent open-channel flows, AIChE Journal, 58(2012), 3867-3877.

[8] Komori S., R. Nagaosa, and H. Ueda, The relationship between surface-renewal and bursting motions in an open-channel flow, J. Fluid Mech., 203(1989), 103-123.
[9] Dong Y.H. and Lu X.Y., Direct numerical simulation of stably and unstably stratified turbulent open channel flows, Acta Mechanica, 177(2005), 115-136.
[10] Teraoka, R., Y. Sugihara, T. Nakagawa and N. Matsunaga, Numerical study on free-surface turbulence in thermally-stratified open-channel flows. Journal of Japan Society of Civil Engineers, B1 (Hydraulic Engineering), 71(2015), 583-588. (In Japanese)
[11] Robinson, S.K., Coherent motions in the turbulent boundary ayer, Annu. Rev. Fluid Mech., 23(1991), 601-639.
[12] Tsumori, H. and Sugihara, Y., Lengthscales of motion that control the air-water gas transfer in grid-stirred turbulence, J. Marine Systems, 66(2007), 6-18.